Nanomaterials

DOI: 10.1002/anie.201001521

Aqueous-Phase Synthesis of Single-Crystal Ceria Nanosheets**

Taekyung Yu, Byungkwon Lim, and Younan Xia**

Two-dimensional (2D) anisotropic nanostructures of metal oxides and semiconductors, especially ultrathin nanosheets (thicknesses < 5 nm), have attracted tremendous attention because of their unusual properties derived from exceptionally small thickness and possible quantum size effects.[1] Typical methods for preparing nanosheets mainly involve the delamination of layer-structured materials.[2] The difficulty in solution-phase synthesis of free-standing nanosheets most likely arises from the fact that metal oxides and semiconductors with a cubic crystal structure, including ceria (CeO_2), have no intrinsic driving force for 2D anisotropic growth. Although it has been shown that nanocrystals made of semiconductors, such as CdTe and CdSe, can self-organize into free-standing nanosheets in a solution phase, they remained assemblies of nanocrystals with an overall polycrystalline structure even after ageing for a long period of time (ca. one month).[3] The solution-phase synthesis of single-crystal nanosheets has met with limited success and still remains a grand challenge.

Ceria has been widely used in catalysis, solid oxide fuel cells, oxygen sensors, and chemical mechanical planarization processes.[4] Nanocrystals of ceria are of particular interest owing to an increased oxygen vacancy that promotes catalytic activity.[5] Ceria nanocrystals have been synthesized by various methods, such as solution precipitation,[6] solvothermal synthesis,[7] microemulsion,[8] microwave-assisted heating,[9] and sonochemical treatment.[10] However, the products of these syntheses have been restricted to nanocrystals with polyhedral structures. Recently, one-dimensional ceria nanostructures, such as nanowire and nanorod, have been synthesized by a nonhydrolytic sol–gel process or alcohothermal route.[11,12] However, 2D nanosheets of ceria have not been reported and, as a result, the influence of quantum size effects on the properties of 2D ceria nanostructures remains largely unexplored.

Here we describe a simple, aqueous route to the synthesis of ultrathin, single-crystalline ceria nanosheets with a thickness of approximately 2.2 nm and lateral dimension up to 4 μm. Our simple synthetic protocol involves the slow, continuous addition of cerium(III) nitrate into an aqueous solution containing 6-aminohexanoic acid (AHA) using a syringe pump at 95 °C. Interestingly, we found that the ceria nanosheets were formed through 2D self-organization of initially formed small ceria nanocrystals, followed by an in situ recrystallization process. To our knowledge, this is the first report of a synthesis of ceria nanosheets with a thickness as thin as approximately 2 nm.

Figures 1 a–d display transmission electron microscopy (TEM) and atomic force microscopy (AFM) images of the as-synthesized ceria nanosheets, clearly showing the formation of nanosheets with lateral dimensions up to 4 μm. Some of the nanosheets appeared to be self-folded (Figure 1 c), indicating that the nanosheets formed in the solution rather than on the substrate during the preparation of the sample for microscopy analysis. The AFM analysis revealed that the nanosheets had a thickness of approximately 2.2 nm (Figure 1 d). A total height of approximately 4.4 nm was also found during the measurements (see Figure S1 in the Supporting Information), which corresponds to the height of a bi-layered nanosheet. The powder X-ray diffraction (XRD) pattern (Figure 1 e) taken from the ceria nanosheets confirmed their cubic fluorite structure (*Fm*3*m*, $a = 5.4113$ Å, JCPDS Card No. 34-0394). A high-resolution TEM (HRTEM) image taken from the top face of a single nanosheet revealed that the lattice fringes were perfectly aligned across the entire surface (Figure 1 f). The corresponding FT pattern showed an array of spots with a sixfold rotational symmetry (Figure 1 f, inset), which can be indexed as the {220} reflections. These data indicate that the nanosheet is a piece of single crystal with its top and bottom faces being enclosed by the {111} surfaces.

To elucidate the formation mechanism of the ceria nanosheets, an aliquot of the reaction solution was taken out at the early stage ($t = 15$ min) and examined by using electron microscopy. In this sample, small ceria nanocrystals with sizes of 2–2.5 nm were observed in great abundance (Figure 2 a). These nanocrystals had a single-crystal structure, as revealed by the HRTEM image in Figure 2 b. Interestingly, we also observed the formation of polycrystalline nanosheets at this reaction stage, as shown in Figure 2 c, d. The similarity between the diameters of the small ceria nanocrystals in Figure 2 b and the single-crystalline domains in a polycrystalline nanosheet in Figure 2 d suggests that the nanosheet was initially formed as a 2D network of ceria nanocrystals. The polycrystalline nanosheets can be considered as intermediate states in the transition from nanocrystals to single-crystal nanosheets. It has been shown by both experiments and simulations that epitaxial reorientation can occur during the sintering of randomly oriented particles, which is driven by the relaxation of the stress resulting from a mis-orientation at

[*] Dr. T. Yu, Dr. B. Lim, Prof. Y. Xia
Department of Biomedical Engineering
Washington University
Saint Louis, MO 63130 (USA)
E-mail: xia@biomed.wustl.edu
limb@seas.wustl.edu

[**] This work was supported in part by the NSF (DMR-0804088) and startup funds from Washington University in St. Louis. T.Y. was also partially supported by the National Research Foundation of Korea (NRF-2009-352-D00160). Part of the work was conducted at the Nano Research Facility (NRF), a member of the National Nanotechnology Infrastructure Network (NNIN), which is supported by the National Science Foundation under Award no. ECS-0335765.

Supporting information for this article is available on the WWW under http://dx.doi.org/10.1002/anie.201001521.

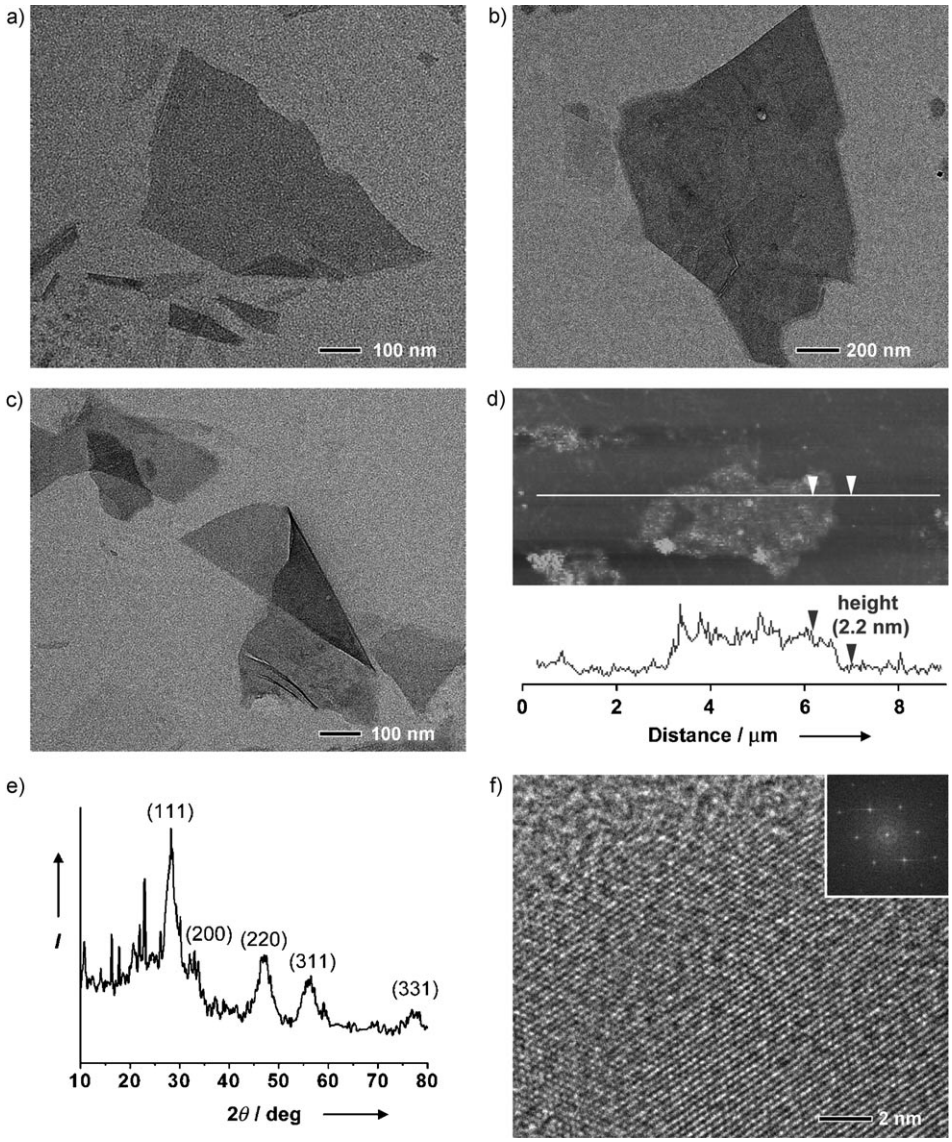

Figure 1. Characterization of ceria nanosheets. a, b) TEM images of nanosheets with different sizes. c) TEM image of a self-folded nanosheet. d) Tapping-mode AFM image and the height along the line shown in the AFM image. e) Powder XRD pattern. f) HRTEM image and the corresponding FT pattern (inset).

the attachment interface.[13] A similar process may occur in the entire nanocrystals embedded in initially assembled, polycrystalline ceria nanosheets, leading to their transition to single-crystalline products.

In our synthesis, the slow addition of a cerium(III) nitrate precursor using a syringe pump is critical to the formation of ceria nanosheets. When the synthesis was conducted by rapidly injecting cerium(III) nitrate with a pipette instead of a syringe pump with other experimental parameters being kept the same as in Figure 1, the product consisted of discrete nanocrystals with a broad size distribution between 5 and 10 nm (Figure 3a). A relatively higher initial concentration of the cerium(III) nitrate precursor could facilitate the rapid growth of nanocrystal seeds into large sizes. Instead of forming self-assembled structures, these ceria nanocrystals further evolved into octahedrons with prolonged reaction time (Figure 3b), which could occur by Oswald ripening. The absence of aggregation for the large ceria nanocrystals can be attributed to an increased colloidal stability resulting from their lower surface energy per volume due to a smaller surface-to-volume ratio. Our results indicate that the generation of nanocrystals with extremely small sizes is a prerequisite for the formation of nanosheets.

Previous studies based on Monte Carlo simulations have shown that a balance of the anisotropic hydrophobic attraction and the electrostatic interactions governs the spontaneous organization of nanocrystals into nanosheets.[3,14] These parameters are also believed to play key roles in the 2D self-organization of ceria nanocrystals. As a part of efforts to obtain a better understanding of the self-organization process, we conducted the reaction in the presence of 0.25 mmol of NaCl, with other experimental parameters being kept the same as in Figure 1. The increased ionic strength of the solution is expected to screen the electrostatic repulsion between the AHA-stabilized ceria nanocrystals. In this synthesis, large spherical aggregates were obtained as the final product (see Figure S2 in the Supporting Information), indicating that a decrease of the electrostatic repulsion between the ceria nanocrystals led to their random aggregation into 3D spheres rather than 2D sheets. These results demonstrate that the electrostatic repulsion is one of essential parameters for 2D self-organization of ceria nanocrystals. At the present time, however, the driving forces for such a 2D self-organization process are not fully resolved. A complete understanding of the interactions between small ceria nanocrystals may require further studies through not only experiments but also simulations.

The band gap of metal oxide nanocrystals has a significant impact on their electronic, optical, and catalytic properties. For instance, it has been shown that an increased band gap can enhance the photocatalytic efficiency of metal oxide nanostructures.[15] Figure 4a shows the absorption spectra recorded from aqueous suspensions of two different types of ceria nanostructures, that is, nanosheet and octahedral nanocrystal.

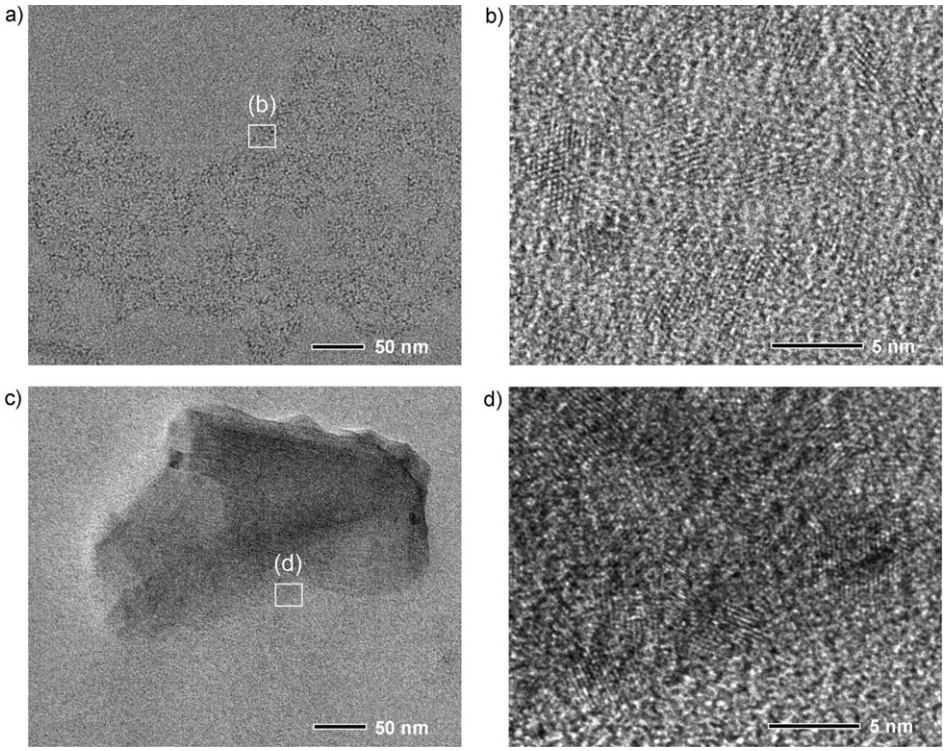

Figure 2. Electron microscopy characterization of the ceria sample prepared under the same conditions as those in Figure 1 except that the reaction time was shortened to 15 min. a) TEM and b) HRTEM images of small ceria nanocrystals with sizes of 2–2.5 nm. c) TEM and d) HRTEM images of a polycrystalline ceria nanosheet.

The absorption in the UV region originates from a charge transfer from O^{2-} to Ce^{4+}, that is, the O 2p→Ce 4f electronic transition. The optical band gap energy (E_g) for direct transitions can be determined from the following relation, $\alpha \propto (h\nu - E_g)^{1/2}/h\nu$, where α is the optical absorption coefficient. Because the optical absorption coefficient (α) is linearly proportional to the absorbance (A) of a sample, the intersection of the extrapolated linear portion in the plot of $(Ah\nu)^2$ versus the photon energy ($h\nu$) gives the band gap energy (E_g) for direct transitions (Figure 4b). The measured band gap was approximately 3.3 eV for the octahedral ceria nanocrystals, which was slightly larger than that of bulk ceria (3.2 eV) due to their relatively small sizes (10–15 nm). Notably, the ceria nanosheets exhibited an unusually large band gap of approximately 3.8 eV, which was even larger than previously reported values (3.3–3.6 eV) for other types of ceria nanostructures, including thin ceria films prepared by an evaporation or sol–gel method and ultrafine ceria particles with sizes of 3–6 nm.[8,16] The increased band gap for the ceria nanosheets indicates the presence of a strong quantum size effect, which is mainly governed by the thickness of the nanosheets rather than their lateral dimensions. Our results clearly show that a band gap of ceria nanostructures can be greatly enlarged by shaping them into nanosheets with an extremely small thickness of only 2 nm.

In summary, we have demonstrated the synthesis of ultrathin, single-crystal ceria nanosheets by a simple, aqueous-phase method. The nanosheets were formed through 2D self-organization of initially formed small ceria nanocrystals and a subsequent recrystallization process. The as-synthesized ceria nanosheets exhibited an unusually large optical band gap energy, which can be attributed to the quantum size effect associated with their extremely small thickness. The ceria nanosheets described in this work hold great potential for fundamental study of their quantum properties.

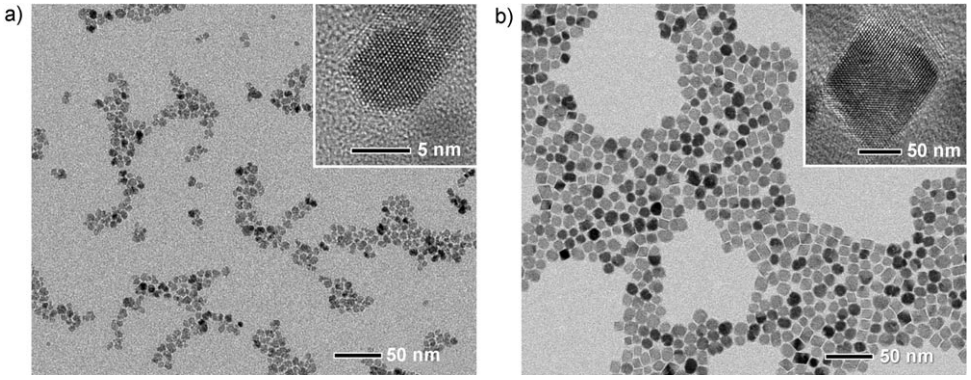

Figure 3. TEM images of the ceria samples prepared under the same conditions as those in Figure 1 except that a cerium(III) nitrate precursor was injected rapidly into the reaction solution using a pipette instead of a syringe pump and the reaction time was 75 min for the sample shown in (a) and 6 h for that in (b). The insets show HRTEM images.

Experimental Section

In a typical synthesis of ceria nanosheets, 6-aminohexanoic acid (AHA, 1 mmol, Aldrich) was dissolved in deionized water (6 mL) and heated to 95 °C in air under magnetic stirring. A small volume of HCl (7 μL, 37 %, Aldrich) was added to the AHA solution to set the solution pH to 5.5. Meanwhile, cerium(III) nitrate hexahydrate ($Ce(NO_3)_3 \cdot 6H_2O$, 0.25 mmol, Aldrich) was dissolved in deionized water (5 mL) at room temperature. Then, the aqueous solution of cerium(III) nitrate was added to the AHA solution using a syringe pump at an injection rate

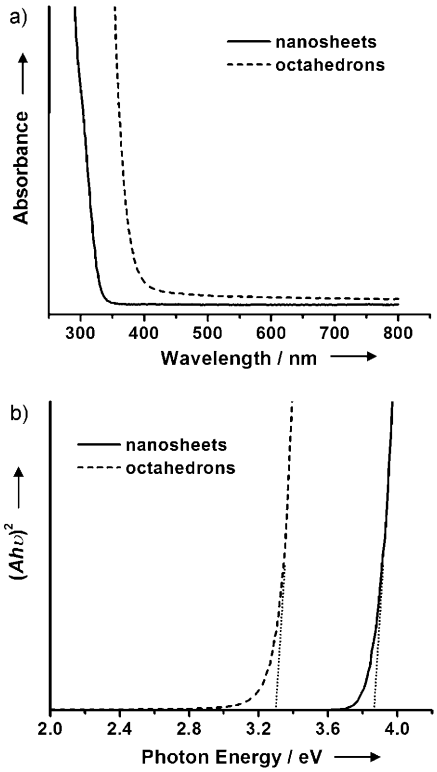

Figure 4. a) UV/Vis spectra of ceria nanosheets (solid line) and octahedral ceria nanocrystals shown in Figure 3b (dashed line). b) Plots of $(Ahv)^2$ versus photon energy (hv).

of 0.083 mL min^{-1}. The reaction mixture was heated at 95 °C in air for 75 min, and cooled down to room temperature.

TEM studies were done with a FEI Tecnai G2 Spirit microscope operated at 120 kV by drop casting the nanoparticle dispersions on carbon-coated copper grids. HRTEM analyses were performed by using a JEOL 2100F microscope operated at 200 kV accelerating voltage. Powder XRD patterns were obtained with a Rigaku D-MAX/A diffractometer at 35 kV and 35 mA. AFM studies were done with a Veeco NanoMan scanning probe microscope at tapping mode. UV/Vis spectra were recorded with a Cary 50 spectrometer (Varian).

Received: March 13, 2010
Published online: May 10, 2010

Keywords: ceria · materials synthesis · nanomaterials · nanosheets · self-assembly

[1] a) M. Osada, Y. Ebina, K. Takada, T. Sasaki, *Adv. Mater.* **2006**, *18*, 295; b) W. Zhang, M. Han, Z. Jiang, Y. Song, Z. Xie, Z. Xu, L. Zheng, *ChemPhysChem* **2007**, *8*, 2091; c) M. Choi, K. Na, J. Kim, Y. Sakamoto, O. Terasaki, R. Ryoo, *Nature* **2009**, *461*, 246; d) J. S. Son, X.-D. Wen, J. Joo, J. Chae, S.-i. Baek, K. Park, J. H. Kim, K. An, J. H. Yu, S. G. Kwon, S.-H. Choi, Z. Wang, Y.-W. Kim, Y. Kuk, R. Hoffmann, T. Hyeon, *Angew. Chem.* **2009**, *121*, 6993; *Angew. Chem. Int. Ed.* **2009**, *48*, 6861.

[2] a) X. Li, G. Zhang, X. Bai, X. Sun, X. Wang, E. Wang, H. Dai, *Nat. Nanotechnol.* **2008**, *3*, 538; b) Y. Hernandez, V. Nicolosi, M. Lotya, F. M. Blighe, Z. Sun, S. De, I. T. McGovern, B. Holland, M. Byrne, Y. K. GunKo, J. J. Boland, P. Niraj, G. Duesberg, S. Krishnamurthy, R. Goodhue, J. Hutchison, V. Scardaci, A. C. Ferrari, J. N. Coleman, *Nat. Nanotechnol.* **2008**, *3*, 563.

[3] Z. Tang, Z. Zhang, Y. Wang, S. C. Glotzer, N. A. Kotov, *Science* **2006**, *314*, 274.

[4] a) A. Trovarelli, C. de Lietenburg, M. Boaro, G. Dolcetti, *Catal. Today* **1999**, *50*, 353; b) S. D. Park, J. M. Vohs, R. J. Gorte, *Nature* **2000**, *404*, 265; c) T. S. Stefanik, H. L. Tuller, *J. Eur. Ceram. Soc.* **2001**, *21*, 1967; d) V. V. Kharton, F. M. Figueiredo, L. Navarro, E. N. Naumovich, A. V. Kovalevsky, A. A. Yaremchenko, A. P. Viskup, A. Carneiro, F. M. B. Marques, J. R. Frade, *J. Mater. Sci.* **2001**, *36*, 1105; e) G. Panzera, V. Modafferi, S. Candamano, A. Donato, F. Frusteri, P. L. Antonucci, *J. Power Sources* **2004**, *135*, 177; f) S. K. Tadokoro, T. C. Porfirio, R. Muccillo, E. N. S. Muccillo, *J. Power Sources* **2004**, *130*, 15; g) X. Feng, D. C. Sayle, Z. L. Wang, M. S. Paras, B. Santora, A. C. Sutorik, T. X. T. Sayle, Y. Yang, Y. Ding, X. Wang, Y.-S. Her, *Science* **2006**, *312*, 1504.

[5] a) S. Deshpande, S. Patil, S. Kuchibhatla, S. Seal, *Appl. Phys. Lett.* **2005**, *87*, 133113; b) C. Korsvik, S. Patil, S. Seal, W. T. Self, *Chem. Commun.* **2007**, 1056; c) X. Liu, K. Zhou, L. Wang, B. Wang, Y. Li, *J. Am. Chem. Soc.* **2009**, *131*, 3140.

[6] a) A. S. Deshpande, N. Pinna, P. Beato, M. Antonietti, M. Niederberger, *Chem. Mater.* **2004**, *16*, 2599; b) H. Chen, H. Chang, *Ceram. Int.* **2005**, *31*, 795.

[7] M. Inoue, M. Kimura, T. Inui, *Chem. Commun.* **1999**, 957.

[8] T. Masui, K. Fujiwara, K. I. Machida, G. Y. Adachi, *Chem. Mater.* **1997**, *9*, 2197.

[9] a) H. Wang, J. J. Zhu, J. M. Zhu, X. H. Liao, S. Xu, T. Ding, H. Y. Chen, *Phys. Chem. Chem. Phys.* **2002**, *4*, 3794; b) F. Bondioli, A. M. Ferrari, L. Lusvarghi, T. Manfredini, S. Nannarone, L. Pasquali, G. Selvaggi, *J. Mater. Chem.* **2005**, *15*, 1061.

[10] L. X. Yin, Y. Q. Wang, G. S. Pang, Y. Koltypin, A. Gedanken, *J. Colloid Interface Sci.* **2002**, *246*, 78.

[11] T. Yu, J. Joo, Y. I. Park, T. Hyeon, *Angew. Chem.* **2005**, *117*, 7577; *Angew. Chem. Int. Ed.* **2005**, *44*, 7411.

[12] a) R. Si, Y.-W. Zhang, L.-P. You, C.-H. Yan, *J. Phys. Chem. B* **2006**, *110*, 5994; b) N. Du, H. Zhang, B. Chen, X. Ma, D. Yang, *J. Phys. Chem. C* **2007**, *111*, 12677.

[13] a) H. Zhu, R. S. Averback, *Philos. Mag. Lett.* **1996**, *73*, 27; b) M. Yeadon, M. Ghaly, J. C. Yang, R. S. Averback, J. M. Gibson, *Appl. Phys. Lett.* **1998**, *73*, 3208.

[14] Z. Zhang, Z. Tang, N. A. Kotov, S. C. Glotzer, *Nano Lett.* **2007**, *7*, 1670.

[15] a) J. Lin, J. C. Yu, D. Lo, S. K. Lam, *J. Catal.* **1999**, *183*, 368; b) J. C. Yu, L. Zhang, J. Yu, *Chem. Mater.* **2002**, *14*, 4647; c) J. Joo, S. G. Kwon, T. Yu, M. Cho, J. Lee, J. Yoon, T. Hyeon, *J. Phys. Chem. B* **2005**, *109*, 15297.

[16] a) K. B. Sundaram, P. Wahid, *Phys. Status Solidi B* **1990**, *161*, K63; b) Z. C. Orel, B. Orel, *Phys. Status Solidi B* **1994**, *186*, K33; c) T. Masui, K. Machida, T. Sakata, H. Mori, G. Adachi, *J. Alloys Compd.* **1997**, *256*, 97.

